Submitted to Nuclear Physics

LBL-1223
Preprint

ROTATIONAL STATES IN ^{171}Hf

I. Rezanka, J. O. Rasmussen, F. M. Bernthal,
C. T. Alonso, J. R. Alonso, S. Hultberg and H. Ryde

August 1972

AEC Contract No. W-7405-eng-48

LBL-1223

DISCLAIMER

ROTATIONAL STATES IN ^{171}Hf*

I. Rezanka, J. O. Rasmussen††, F. M. Bernthal†, C. T. Alonso†† and J. R. Alonso††

Heavy Ion Accelerator Laboratory
Yale University

and

S. Hultberg and H. Ryde

Research Institute for Physics
Stockholm

August 1972

Abstract

Alpha-particle irradiation of an enriched ytterbium target and ^{10,11}B irradiation of a holmium target were used to populate excited states in ^{171}Hf. Rotational bands built on the $7/2^+[633]$, $5/2^-[512]$ and $1/2^-[521]$ Nilsson states were followed up to levels with spins 29/2, 25/2, and 29/2, respectively. The observed energy levels and transition probabilities are compared with the predictions of the rotational model and with the results of a Coriolis coupling calculation.

NUCLEAR REACTIONS: ^{170}Yb(α,3n), E = 20-43 MeV; ^{165}Ho(^{10}B,4n), E = 45-60 MeV; ^{165}Ho(^{11}B,5n), E = 50-75 MeV; measured $\sigma(E,E_\gamma,\theta)$, E_γ, I_γ, γγ coincidences. Enriched Yb target. ^{171}Hf deduced levels, I, π, K, E2/M1, $(g_K - g_R)$. Coriolis calculations.

*This work was partly supported by the U. S. Atomic Energy Commission.

†Present address: Chemistry Department, Michigan State University, East Lansing, Michigan, 48823.

††Present address: Lawrence Berkeley Laboratory, University of California, Berkeley, California, 94720.

1. Introduction

In a preceding paper[1]) a study of the rotational states in the odd-mass isotopes $^{173-177}$Hf populated in (α,xn) reactions was reported by some of the authors of this work. It seemed highly desirable to extend that study to more neutron-deficient hafnium isotopes, since the distortions found in even-parity bands are expected to be more pronounced for the lighter isotopes. In order to accomplish this, certain experimental and practical problems had to be overcome: (a) isotopically enriched targets for (α,xn) reactions had to be prepared, (b) the results of transfer particle reactions, which proved to be so vital for the correct interpretation of the structure of the heavier isotopes[1]), were missing, and (c) earlier radioactivity studies were scarce. On the other hand, the lighter hafnium isotopes can also be produced in (Heavy Ion,xn) reactions, providing a useful alternate means of production. Therefore, the experimental work on the structure of ^{171}Hf was performed in parallel in Stockholm at the Research Institute for Physics using the methods of (α,xn) reactions and at the Yale Heavy Ion Accelerator employing (HI,xn) reactions. The authors feel that it is desirable to join their efforts in interpretation of these data and to publish the results in one joint paper. In addition, a study of the decay of ^{171}Ta leading to the low-lying states of ^{171}Hf is now being finished at Yale, and preliminary results which were published in ref.[2]) are used for the assignments of the lower members of the rotational bands. Preliminary results of our in-beam study of ^{171}Hf were included in ref.[3]).

2. Experimental Procedure and Results

Ytterbium metal, enriched to 81% in ^{170}Yb and rolled into a self-supporting foil of 5 mg/cm^2, was used as a target for the α-particle irradiations. The

isotopic composition of this target is shown in Table 1. For the irradiations with boron ions, a 99.9% pure metallic holmium foil was rolled into a self-supporting target 7 mg/cm^2 thick.

Alpha-particles from the Stockholm 225-cm cyclotron were used for the production of ^{171}Hf in the first part of the study. An experimental arrangement similar to that described in refs.[4,5]) was used for this part of the study. Ions of ^{10}B and ^{11}B, accelerated in the Yale Heavy Ion Accelerator (HIA), were employed for the second part of the study. This experimental set-up has also been described in an earlier publication[6]). The following experiments were performed in this study.

(1) The yield of γ-rays was followed as a function of the beam energy--from 20 to 43 MeV for α particles, from 45 to 60 MeV and from 50 to 75 MeV for ^{10}B and ^{11}B ions, respectively. In this way, one can clearly distinguish the radiations originating in reactions with emission of different numbers of neutrons, e.g., the (α,3n) reaction from the (α,2n) and (α,4n) reaction. To a lesser degree, these relative excitation functions of γ-rays are sensitive to the spin values of the levels involved. The optimum energy for the reaction leading to ^{171}Hf was found to be 38 MeV for the ^{170}Yb(α,3n)^{171}Hf reaction and 52 MeV and 68 MeV for the ^{165}Ho(^{10}B,4n)^{171}Hf and ^{165}Ho(^{11}B,5n)^{171}Hf reactions, respectively. Several Ge(Li) detectors with active volumes ranging from 15 to 43 cm^3 were used for these measurements. The resolution of these detectors was 1.3-2.0 keV at 200 keV. The energies, determined from simultaneous measurement with standard radioactive sources, are accurate to 0.1 keV for the strongest γ-lines (with intensities of 20 and higher in the units of Table 1), to 0.2 keV for the weaker lines (with intensities between 5 and 20) and to 0.4 keV for the rest of the lines. The intensities are considered to be correct within 10% for

the first group of more intense γ-lines and within 20% for the rest. The γ-ray spectrum from the reaction with α-particles is shown in fig. 1, and the spectrum from the ^{10}B bombardment work in fig. 2. Both spectra were taken at the mentioned optimum energies. The information concerning the γ-ray lines of ^{171}Hf observed in these reactions is summarized in Table 2.

(2) The angular distributions of the γ-rays were obtained by measuring the intensities of the lines at different angles with respect to the direction of the beam. The X-ray peaks, composed of the K-lines of both the target and the products of the reactions, were used as isotropic intensity reference. The beam was stopped close to the target in the ^{10}B irradiations and the measurement was done at three angles: 0°, 55°, and 90°. In the α-particle experiment, the beam was stopped considerably farther downstream so that angles near 0° were not available for measurement; the angles used were 150°, 125°, 110° and 90°. In this latter case two surface barrier Si detectors, placed symmetrically at 25° with respect to the beam and registering the elastically scattered α-particles, were employed as an alternative way of normalization. This normalization and the one using the X-ray peak were found to be compatible within the experimental errors. The angular distribution results are included in Table 2.

(3) During the investigations at the Yale HIA a γγ coincidence experiment was performed, using two Ge(Li) detectors with active volumes of 15 and 40 cm^3. The coincidences were recorded event-by-event on a magnetic tape. The experimental set-up, data acquisition and subsequent analysis were the same as described in ref.[7]). A total of 2×10^5 coincidence counts were accumulated. Parts of some coincidence spectra which were restored after the experiment from the magnetic tape are shown in fig. 3. The coincidence relationships established in this experiment are summarized in Table 3.

3. Rotational Band Assignment

One has difficulty in assigning the observed transitions to the rotational bands in ^{171}Hf because very little is known about the states in this nucleus from other methods. The availability of such data proved to be very important for the in-beam study of the heavier hafnium isotopes[1]). The neighboring even nucleus ^{172}Hf is not stable and thus the one-neutron transfer reaction leading to ^{171}Hf is not feasible. Until recently, the radioactive decay of ^{171}Ta to the levels of ^{171}Hf was not known. Even at the present time, only gross features of the ^{171}Ta decay are available from published works[2,8]) and no level scheme has so far been proposed. However, a detailed study of the ^{171}Ta decay scheme is in progress at Yale (cf. preliminary publication[2])), and we take advantage of this information in establishing the level structure of ^{171}Hf. The part of the ^{171}Hf level scheme which was determined from this radioactivity study and which overlaps with our level scheme is shown in fig. 4. It can be seen that one important question about the very lowest excited states still remains unanswered, that is, the excitation energy of $1/2^-[521]$ band head. Nevertheless, the existence of the three single-particle states, $1/2^-[521]$, $7/2^+[633]$, and $5/2^-[512]$, was firmly established from this study of ^{171}Ta radioactivity, together with several excited levels built on these states.

The results from the in-beam study were in good agreement with the level scheme of fig. 4. Based on all the information described in Section 2, we are able to identify the rotational bands up to $29/2^+$ for the $7/2^+$ band head, up to $25/2^-$ for the $1/2^-[521]$ band head, and up to $23/2^-$ for the $5/2^-[512]$ band head. The level scheme as determined in this study is shown in fig. 5.

4. Discussion

4.1 ODD-PARITY BANDS

The two odd-parity bands observed in this study, $1/2^-[521]$ and $5/2^-[512]$, can be sufficiently well described by the rotational formula[9,10]

$$E_{rot} = A\{I(I+1) - K^2\} + B\{I(I+1) - K^2\}^2 + C\{I(I+1) - K^2\}^3 + \ldots + (-1)^{I+K} \prod_{i=I-K}^{K} (I+i)\{A_{2K} + B_{2K}[I(I+1) - K] + \ldots\} \quad (1)$$

Using the least squares method it is possible to fit the observed rotational levels in these two bands almost to within the experimental errors. At the same time, the contributions originating in the highest order member of this truncated expansion are small even for the levels with highest spin. The results of this computer fit are shown in Table 4.

It should be noted that the decoupling factor of + .76 ($= A_{2K}/A$) for the $K = 1/2^-$ band is somewhat less than the prediction of the Nilsson model, but as can be seen from fig. 16 of the compilation[11] by Dzhelepov, Dranitsyna, and Mikhailov, our measured value falls within the cluster of a values in this mass region.

The results from angular distribution measurements and the branching ratios can be combined in order to obtain information about the M1-E2 mixing amplitudes δ and consequently about the gyromagnetic ratios. The branching ratios generally yield more accurate values of δ but cannot determine its sign; on the other hand, the angular distributions determine the sign of δ unequivocally, and its absolute value rather poorly. This situation is reflected in the data of Table 5. The experimental values of the pure E2 transitions ($I \rightarrow I - 2$) compared with the theoretical values calculated for complete alignment[14] yield the

attenuation factor for a particular level. This factor is then used to correct the angular distribution of the mixed $I \rightarrow I - 1$ transition and the value of δ was obtained from comparison of this corrected experimental value with the theoretical one[14]). The differences between the intrinsic and rotational gyromagnetic ratios $g_K - g_R$ shown also in Table 5 were obtained by combining the information of these two kinds for the $5/2^-[512]$ band and using the value of 7.1 barns for the quadrupole moment of the core. The latter value was extrapolated from the neighboring even nuclei[15]). Adopting the value of 0.3 for the gyromagnetic ratio of the core leads to values of g_K that are within experimental errors of the values calculated in ref.[21]) where the procedure yielded values of about -0.32 for g_K. In these calculations a value of 0.6 was used for g_s. The possible exception is the $9/2^-$ state at 258.5 keV. For this state, however, the intensity of the cross-over 208.6 keV transition is known rather inaccurately.

4.2 EVEN PARITY BAND $7/2^+[633]$; COMPARISON WITH OTHER HAFNIUM ISOTOPES

Even from a visual inspection of the spectrum of the $7/2^+[633]$ band, large deviations from the rotational spacings are apparent. This irregularity is even more apparent when the spacing in the band divided by spin value is plotted against the square of the spin (fig. 6). Since the perturbation, which is caused by a Coriolis coupling, is so large, it is unreasonable to expect an expansion formula such as eq. 1 to accurately describe the band.

The usual theoretical treatment of these highly perturbed unique parity bands consists of the numerical diagonalization of the secular determinant of the Coriolis interaction. The diagonalization is normally performed in the space of one-quasi particle Nilsson states all originating in one spherical shell model orbital; in this case, the shell model state is $i_{13/2}$ and the corresponding Nilsson states extend from

$1/2^+[660]$ to $13/2^+[606]$. Such methods were applied to a number of cases (see, e.g., refs.[16,13,12]) as well as to the odd-mass hafnium nuclei in ref.[1]).

Here, the modified theoretical approach of C. T. Alonso and J. O. Rasmussen[17]) is tested and applied not only to the unique parity band in ^{171}Hf but to the whole series of odd-mass hafnium nuclei $^{171-179}$Hf. The method, called by its authors the "supermatrix" method, is briefly outlined below.

The importance of the supermatrix technique lies in its more detailed treatment of the pairing interaction than is afforded by the usual smaller basis, where Coriolis matrix elements are merely attenuated by factors involving u and v, the BCS amplitudes. Instead of the usual quasi-particle energy expression for the band heads in an n×n matrix, viz.

$$E_o = \sqrt{(\varepsilon_i - \lambda)^2 + \Delta^2} - \Delta \qquad (2)$$

which tends to overestimate pairing effects, the independent particle energy expression

$$E_o = |\varepsilon_i - \lambda| \pm E_{h,p} \qquad (3)$$

is used in a 2n×2n "supermatrix". In this expanded matrix the Nilsson energies ε_i are theoretically calculated and λ is taken halfway between the last pair-filled level, and the next higher unfilled level of the j-subshell (e.g., $i_{13/2}$) under consideration. The supermatrix is divided into blocks which conserve the number of pairs in the subsystem. The lower right block of rank n is the standard Coriolis matrix using $|\varepsilon_i - \lambda|$ for the band heads, but its restricted meaning here is that states have exactly N nucleons in the j-family of orbitals under treatment, i.e., j^N. The upper left n×n block describes an (N ± 2)-nucleon Coriolis matrix in which a pair has scattered into or out of the j-subshell being considered. The effect of this scattering is to change the band-head energies by

the amount of energy it took the pair to scatter. If pairing were taken into account in the calculation of diagonal energies, E_p and E_h would be functions of K because of blocking by the odd nucleon near the Fermi surface, but in order to minimize the number of parameters we take only two energies, E_p and E_h, as adjustable band-fitting parameters. The states of the same projection Ω in the N and N ± 2 blocks are then connected by off-diagonal elements of the order of the pairing strength G times the effective number of orbitals n participating in the pairing configuration mixing.

For an example of the supermatrix construction in the specific case of ^{177}Hf and I = 9/2, see fig. 7. The ground state of ^{177}Hf is known to be the $7/2^-[514]$ orbital, and the next lowest single particle state is $9/2^+[624]$. Thus, the lower right block represents states with nine neutrons in the $i_{13/2}$ subshell. The upper left block then reflects the fact that two nucleons previously resident in the other low-lying filled $i_{13/2}$ orbitals can be promoted into the unfilled odd-parity orbitals, the lowest of which is the $7/2^-[514]$.

This method was applied to numerical fitting of all of the known $i_{13/2}$ shell model state levels in the hafnium isotopes 171, 173, 175, 177 and 179. For ^{171}Hf, the experimental data of this work are used while for ^{173,175,177}Hf the data from ref.[1]) were taken and for ^{179}Hf the data were from ref.[22]). Also, for ^{177}Hf, the results of refs. [18-20,23]) were included. The experimental and theoretical level energies are listed in Table 6 and values for the various parameters are given in Table 7. Parameters that were calculated theoretically are marked in Table 7 with an asterisk. The remaining parameters were allowed to vary in the tri-diagonalization program Betable developed by Clements at Berkeley[24]). In Table 7, a is the decoupling parameter for the K = 1/2 band

and α is the off-diagonal matrix element reduction factor which has generally been found necessary in Coriolis band fitting of experimental energy levels and in part is due to the uu' + vv" pairing factor.

What can be noted from the trends in parameters as shown in Table 7? First of all, the form of the supermatrix we used is most appropriate for the three central cases, masses 173, 175, and 177, since for them the chemical potential lies between the $7/2^+$ and $9/2^+$ ($i_{13/2}$) orbitals. For these nuclei the ground band has the odd neutron in one of the three odd-parity orbitals lying between the $7/2^+$ and $9/2^+$ orbitals. Here it is most appropriate to take into account in the supermatrix the blocks with N = 7 and N + 2 = 9 neutrons in the $i_{13/2}$ family. However, for ^{171}Hf the $7/2^+$ band is ground, and blocks with 5, 7, and 9 neutrons should have been taken into account. Likewise, for ^{179}Hf, blocks with 7, 9, and 11 neutrons should have been used. For these reasons the best-fit parameters of the extreme cases of mass 171 and 179 have less direct physical significance, and we confine our examination of Table 7 for trends to the three intermediate-mass cases. For these three cases E_p shows a monotonic increase with mass, and except for ^{173}Hf, E_h shows a decreasing magnitude. These trends are those expected from the simple Nilsson level diagram. For these three cases, the values of effective pairing nG_h and nG_p are not very different and could have been constrained to equality without hurting the level fit very much. The magnitudes of the effective pairing parameters are quite reasonable. They should equal the pairing strength G times the effective number of odd-parity orbitals participating in pairing correlation (i.e., $\sum_{\pi odd} u_i v_i$). This sum is approximately Δ/G times the fraction f_o of odd-parity orbital density to total density at the Fermi surface. Thus nG should nearly equal $f_o\Delta$. The

odd-even mass difference for neutrons Δ_n is around 0.6-0.8 MeV in the Hf region, and the fractional odd-parity orbital density is around 2/3. Thus, the best-fit effective pairing parameters in the range of -346 to -724 keV are reasonable.

The values of decoupling parameter a are near the value 7 for a pure $i_{13/2}$ orbital, but it is hardly to be expected that band-fitting of the K = 7/2 band should be sensitive to the decoupling parameter, since it affects energy spacings in the K = 7/2 band only in the seventh order of the Coriolis interaction.

Coriolis attenuation factors α range from a half to two-thirds, and it is difficult to make a quantitative comparison with theory here, since we are treating some pairing effects explicitly and cannot equate to the ordinary uu' + vv' factor nor to Pyatov's recoil term correction. However, these α factors seem reasonable.

The rotational constants $(\frac{\hbar^2}{2J})$ of the intermediate even nuclei ^{174}Hf and ^{176}Hf are 15.1 and 14.7 keV, respectively. We hoped that the fitted rotational constants of Table 7 would approach these "core" values. (Indeed, one might expect still larger unrenormalized $\frac{\hbar^2}{2J}$ values, since the core is the system of nucleons and orbitals excluding the $i_{13/2}$ set, which is treated explicitly.) We have not yet tried forcing fits with $\frac{\hbar^2}{2J}$ held at or above the even-even values, though that would be a reasonable approach.

For ^{177}Hf there is a more stringent test of the theory in that two levels of a second even-parity band are known. The fit of Table 6 is not very good as regards the rotational spacing in the higher band, and this case deserves further study. Evidently the least squares adjustment is most influenced by the ground band, where many levels are known in contrast to the excited band.

Transition probabilities and magnetic moments may provide further tests of the Coriolis mixed wave functions and the supermatrix variants. However, we have not yet made such comparisons.

The levels are fit on the average to within 1.5 keV. The expanded basis set of the supermatrix does not appear to eliminate the need for an attenuation factor α for Coriolis matrix elements, but it does eliminate the need for arbitrarily cutting down the matrix element connecting the lowest particle and lowest hole bands. The reason that the supermatrix provides a natural effective attenuation of band mixing between the lowest particle and lowest hole bands is because these bands are now connected only in second order through a product of Coriolis and pairing interactions, not in first order by the Coriolis interaction. Pyatov and collaborators[25]) have theoretically studied various effects renormalizing Coriolis matrix elements, and they attribute an over-all reduction to a "recoil" term. Their renormalization affects all Coriolis matrix elements equally. Thus, we see emerging a more satisfactory picture of Coriolis band mixing in which the arbitrariness of selective reduction factors for particular matrix elements or use of different moments-of-inertia for different bands is unnecessary.

Perhaps it might be argued that our improved band-fitting merely follows from the use of more free parameters, although we have left no freedom in adjusting Nilsson energies but have taken them directly from a new computer code including hexadecapole shape parameters due to Nilsson et al.[21]). We feel, however, that the essential physics of the Coriolis band mixing is better handled with our larger basis set than with the usual calculations. Ideally one would like to solve the problem in a very large shell model basis with amplitudes for each configuration of odd particle and pairs. Since such a shell model basis is too large to be practical, the BCS variational approach is used instead. Our supermatrix is one step from BCS toward the larger shell model basis. We are

not yet consistently treating pairing among all orbital combinations but are instead introducing an effective nG pairing matrix element between the top-most unblocked orbitals of opposite parity. Thus, pairing manifests itself in the factor n, the effective number of orbitals participating in pair transfer between the odd and the even parity orbital systems. Pairing modifies E_h and E_p from their lowest order estimates as the energy differences of the lowest lying odd-parity Nilsson orbital and the $9/2^+$ and $7/2^+$ Nilsson orbital energies respectively. Also pairing enters in the factor α, but it is likely that centrifugal and spin-spin polarization effects of Chernej, Baznat, and Pyatov [25]) are also contributors to the reduction of α below unity. Indeed, their numerical calculations for rare earths showed values of polarization factors R_j around 0.7.

We wish to express our appreciation to Robert Hildrich and the crew of the Yale Heavy Ion Accelerator for their invaluable part in providing the needed heavy ion beams. Likewise, the assistance of Dr. Hugo Atterling and the staff of the cyclotron at the Research Institute for Physics, Stockholm, is gratefully acknowledged. We are grateful to Dr. C. F. Tsang for providing the Nilsson orbital energy program and to Mr. S. Y. Chu for adapting and running this program at Yale. Thanks are due to Dr. N. I. Pyatov for discussions of his polarization terms in Coriolis coupling.

REFERENCES

1) S. Hultberg, I. Rezanka and H. Ryde, to be published.

2) I. Rezanka, I.-M. Ladenbauer-Bellis, F. M. Bernthal and J. O. Rasmussen, Phys. Rev. Letts. 25 (1970) 1499.

3) I. Rezanka, S. Hultberg, H. Ryde, J. O. Rasmussen, F. M. Bernthal and J. R. Alonso, Proc. of the International Conference on the Properties of Nuclei Far from the Region of Beta-Stability at Leysin (CERN, Geneva 1970), p. 949.

4) I. Bergstrom, C.-J. Herrlander, A. Kerek and A. Luukko, Nucl. Phys. A123 (1969) 99.

5) S. A. Hjorth, H. Ryde and B. Skånberg, Ark. Fys. 38 (1968) 537.

6) J. Alonso, H. Bakhru, F. M. Bernthal, J. Boutet, B. Olsen, I. Rezanka and J. O. Rasmussen, Nucl. Phys. A160 (1971) 193.

7) I. Rezanka, F. M. Bernthal, J. O. Rasmussen, R. Stokstad, I. Fraser, J. Greenberg and D. A. Bromley, Nucl. Phys. A179 (1972) 51.

8) R. Arlt, Z. Malek, G. Muziol and H. Strusny, Izv. Akad. Nauk SSSR, Ser. Fiz. 33 (1969) 1232.

9) T. Hamamoto and T. Udagawa, Nucl. Phys. A126 (1969) 241.

10) A. Bohr and B. R. Mottelson, Monograph on Nuclear Structure, New York, to be published.

11) B. S. Dzhelepov, G. F. Dranitsyna and V. M. Mikhailov, Svoistva deformirovannych yader (Nauka, Leningrad 1971), p. 150.

12) E. Selin, S. A. Hjorth and H. Ryde, Physica Scripta 2 (1970) 181.

13) T. Lindblad, H. Ryde and D. Barneoud, to be published.

14) T. Yamazaki, Nucl. Data A3 (1967) 1.

15) P. H. Stelson and L. Grodzins, Nucl. Data A1 (1965) 21.

16) S. A. Hjorth, H. Ryde, K. A. Hagemann, G. Løvhøiden and J. C. Waddington, Nucl. Phys. A144 (1970) 513.

17) C. T. Alonso and J. O. Rasmussen, Bull. Am. Phys. Soc. Ser. II, 17 (1972) 579.

18) M. Jorgensen, O. B. Nielsen and G. Sidenius, Phys. Letts. 1 (1962) 321.

19) L. Kirstensen, J. Jorgensen, O. B. Nielsen and G. Sidenius, Phys. Letts. 8 (1964) 57.

20) H. J. Haverfield, F. M. Bernthal and J. M. Hollander, Nucl. Phys. A94 (1967) 337.

21) S. G. Nilsson, C. F. Tsang, A. Sobiczewski, Z. Szymanski, S. Wycech, C. Gustafson, I. Lamm, P. Möller and B. Nilsson, Nucl. Phys. A131 (1969) 1.

22) H. Hübel, R. A. Naumann, M. L. Andersen, J. S. Larsen, O. B. Nielsen and N. O. Roy, Phys. Rev. C1 (1970) 1845.

23) F. A. Rickey, Jr. and R. K. Sheline, Phys. Rev. 170 (1968) 1157.

24) T. C. Clements, private report, Lawrence Radiation Laboratory (Berkeley, 1966).

25) N. I. Pyatov, M. I. Chernej and M. I. Baznat, Preprint E4-5468 (Joint Institute for Nuclear Research, Dubna 1970).

M. I. Chernej, M. I. Baznat and N. I. Pyatov, Preprint E4-5550 (Joint Institute for Nuclear Research, Dubna 1970).

Table 1

Isotopic Composition of the Yb Target Used for the α-particle Bombardment

Mass Number	Percentage
168	< 0.07
170	81.4 ± 0.4
171	7.8 ± 0.2
172	4.8 ± 0.2
173	2.3 ± 0.1
174	3.1 ± 0.1
176	0.73± 0.05

Table 2. Gamma Transitions in ^{171}Hf

E_γ (keV)	I_γ [a] (arb. units) (α,3n)	(^{10}B,4n)	(^{11}B,5n)	Angular Distr. Coeff. A_2/A_0	A_4/A_0	^{171}Hf [b]	Assignment band	levels
81.1	10					A	$1/2^-[521]$	$5/2^- \rightarrow 1/2^-$
84.2	58[c]	[d]		-0.44 ± 0.06	+0.09 ± 0.13	A	$7/2^+[633]$	$11/2^+ \rightarrow 9/2^+$
92.2	35					A	$5/2^-[512]$	$7/2^- \rightarrow 5/2^-$
98.9	48	40		-0.58 ± 0.08	-0.01 ± 0.13	A	$7/2^+[633]$	$13/2^+ \rightarrow 11/2^+$
110.0	5	15				B		
116.7	16			-0.48 ± 0.13	+0.10 ± 0.20	A	$5/2^-[512]$	$9/2^- \rightarrow 7/2^-$
123.6	21					C		
129.7	37	40		-0.75 ± 0.13	+0.02 ± 0.12	A	$7/2^+[633]$	$17/2^+ \rightarrow 15/2^+$
137.0	58	65	30	-0.76 ± 0.11	-0.10 ± 0.15	A	$7/2^+[633]$	$15/2^+ \rightarrow 13/2^+$
139.7	19			-0.26 ± 0.08	+0.11 ± 0.20	A	$5/2^-[512]$	$11/2^- \rightarrow 9/2^-$
145.9	21					A	$7/2^+[633]$	$11/2^+ \rightarrow 7/2^+$
148.9	23	31		-0.32 ± 0.19		A	$7/2^+[633]$	$21/2^+ \rightarrow 19/2^+$
160.2	2					B	$7/2^+[633]$	$25/2^+ \rightarrow 23/2^+$
162.0	15			-0.58 ± 0.11	-0.01 ± 0.15	A	$5/2^-[512]$	$13/2^- \rightarrow 11/2^-$
165.5	29	33		+0.30 ± 0.15		A	$1/2^-[521]$	$7/2^- \rightarrow 3/2^-$
174.9	66	71	52	+0.18 ± 0.13		A	$1/2^-[521]$	$9/2^- \rightarrow 5/2^-$
180.7	12			-0.40 ± 0.21	+0.07 ± 0.25	A	$5/2^-[512]$	$15/2^- \rightarrow 13/2^-$
183.3	71	87	75	+0.31 ± 0.11		A	$7/2^+[633]$	$13/2^+ \rightarrow 9/2^+$

(continued)

Table 2. (continued)

E_γ (keV)	I_γ [a] (arb. units) (α,3n)	(^{10}B,4n)	(^{11}B,5n)	Angular Distr. Coeff. A_2/A_0	A_4/A_0	^{171}Hf [b]	Assignment band	levels
190.3	12			0.00 ± 0.09	+0.01 ± 0.10	B		
198.9	5					B	5/2⁻[512]	17/2⁻ → 15/2⁻
203.7	27	32		-0.61 ± 0.12		A	7/2⁺[633]	19/2⁺ → 17/2⁺
208.6	10					B	5/2⁻[512]	9/2⁻ → 5/2⁻
224.9	3					B	5/2⁻[512]	21/2⁻ → 19/2⁻
236.0	95	113	87	+0.36 ± 0.09	+0.05 ± 0.12	A	7/2⁺[633]	15/2⁺ → 11/2⁺
253.0	30	34		+0.38 ± 0.11		A	1/2⁻[521]	11/2⁻ → 7/2⁻
256.3	15			+0.30 ± 0.10	-0.07 ± 0.20	A	5/2⁻[512]	11/2⁻ → 7/2⁻
258.3	73	101	95	+0.33 ± 0.14	+0.02 ± 0.21	A	1/2⁻[521]	13/2⁻ → 9/2⁻
267.2	118	137	97	+0.27 ± 0.10	-0.06 ± 0.19	A	7/2⁺[633]	17/2⁺ → 11/2⁺
274.2	6					C		
278.9	12	21		-0.30 ± 0.15		A	7/2⁺[633]	23/2⁺ → 21/2⁺
295.2	25	20				A		
301.7	22	8		+0.38 ± 0.11	+0.03 ± 0.20	A	5/2⁻[512]	13/2⁻ → 9/2⁻ [e]
329.9	95	84	78	+0.36 ± 0.08	-0.06 ± 0.14	A	1/2⁻[521]	17/2⁻ → 13/2⁻ ; 15/2⁻ → 11/2⁻
333.9	100	100	95	+0.46 ± 0.13	+0.06 ± 0.15	A	7/2⁺[633]	19/2⁺ → 15/2⁺
342.6	19	16		+0.39 ± 0.09	0.00 ± 0.13	A	5/2⁻[512]	15/2⁻ → 11/2⁻
346.5	15					A		
354.0	98	84	79	+0.36 ± 0.08	-0.02 ± 0.13	A	7/2⁺[633]	21/2⁺ → 17/2⁺

(continued)

Table 2. (continued)

E_γ (keV)	I_γ[a] (arb. units) (α,3n)	(^{10}B,4n)	(^{11}B,5n)	Angular Distr. Coeff. A_2/A_0	A_4/A_0	^{171}Hf[b])	Assignment band	levels
365.0	7					C		
367.6	8					B	$1/2^-[521]$	$19/2^- \rightarrow 17/2^-$
379.3	20			+0.46 ± 0.12	+0.07 ± 0.17	A	$5/2^-[512]$	$17/2^- \rightarrow 13/2^-$
389.7	52	45	39	+0.42 ± 0.11	-0.01 ± 0.13	A	$1/2^-[521]$	$21/2^- \rightarrow 17/2^-$
395.5	18			+0.38 ± 0.09	-0.07 ± 0.14	A	$1/2^-[521]$	$19/2^- \rightarrow 15/2^-$
406.0	5					B		
412.0	15	20				A	$5/2^-[512]$	$19/2^- \rightarrow 15/2^-$
429.0	69	57	61	+0.40 ± 0.10	-0.04 ± 0.13	A	$7/2^+[633]$	$23/2^+ \rightarrow 19/2^+$
438.2	16	18		+0.54 ± 0.22		A	$5/2^-[512]$ $1/2^-[521]$	$21/2^- \rightarrow 17/2^-$ $25/2^- \rightarrow 21/2^-$
440.0	100	100	100	+0.52 ± 0.19	+0.10 ± 0.23	A	$7/2^+[633]$	$25/2^+ \rightarrow 21/2^+$
447.4	8			+0.55 ± 0.24		B	$1/2^-[521]$	$23/2^- \rightarrow 19/2^-$
454.0	17	20		+0.48 ± 0.17		A	$5/2^-[512]$	$23/2^- \rightarrow 19/2^-$
461.9	14	18		+0.21 ± 0.10		A	$1/2^-[521]$	$29/2^- \rightarrow 25/2^-$
469.5	12					B	$5/2^-[512]$	$25/2^- \rightarrow 21/2^-$
478.2	4					C		
485.3	25[f])			+0.52 ± 0.20	+0.02 ± 0.30	C		
498.0	9					A		
507	30					B		
516.1	37	33	27	+0.50 ± 0.18		A	$7/2^+[633]$	$27/2^+ \rightarrow 23/2^+$

(continued)

Table 2. (continued)

E_γ	I_γ[a] (arb. units)			Angular Distr. Coeff.			Assignment	
(keV)	(α,3n)	^{10}B,4n)	(^{11}B,5n)	A_2/A_0	A_4/A_0	^{171}Hf[b])	band	levels
521.7	35	23		+0.38 ± 0.10		A	$7/2^+[633]$	$29/2^+ \rightarrow 25/2^+$
527.6	11			+0.33 ± 0.12		A		
540.3	6					B		
557.5	8					A		
569.3	4					B		
571.8	4					B		
576.5	3					B		
592.7	15					B		
666.6	5					B		

[a]) The intensities were determined at an angle of 125° with respect to the beam direction, and for the optimum beam energies: α-particles - 39 MeV, ^{10}B - 54 MeV, ^{11}B - 70.5 MeV.

[b]) Confidence rating of the assignment to ^{171}Hf: A - certain, B - highly probable, C - doubtful.

[c]) Admixture of ^{170}Yb target excitation may be present.

[d]) Observed with ^{10}B beam in the coincidence experiment only.

[e]) Small part of the line intensity may be due to the $15/2^- \rightarrow 13/2^-$ transition in the $1/2^-[521]$ band.

[f]) Not completely resolved from the 483.6 keV transition in ^{172}Hf.

Table 3

Coincidence Relations Between the γ-rays in ^{171}Hf Excited by the $^{165}Ho(^{10}B,4n)$ Reaction

E_γ (keV)	98.9	137.0	258.3	333.9
84.2	X	X		
98.9		X		
174.9			X	
236.0				X

Table 4

Rotational Parameters of the

$1/2^-[521]$ and $5/2^-[512]$ Bands in ^{171}Hf

Band	A (keV)	B (eV)	C (MeV)	A_{2K} (keV)	B_{2K} (eV)
$1/2^-[521]$	+12.52 ± 0.05	-14.9 ± 0.5	+20 ± 2	+9.51 ± 0.09	-9 ± 2
$5/2^-[512]$	+13.28 ± 0.03	-11.6 ± 0.4	+4.6 ± 1.0	$(+1.3 \pm 1.2) \times 10^{-6}$	

Table 5

Gyromagnetic Ratios $g_K - g_R$ for the $5/2^-[512]$ Band in ^{171}Hf. The Value of 7.1 barn was Adopted for Q_o.

Initial spin	Mixing Amplitude from angular distribution	Mixing Amplitude from branching ratio	$g_K - g_R$
9/2	from -0.04 to -4.0	0.41 ± 0.05	-0.43 ± 0.08
11/2	from +0.05 to -0.25 or from -3.0 to 10.0	0.23 ± 0.04	-0.73 ± 0.12
13/2	from -0.08 to -0.35 or from -2.0 to -5.0	0.24 ± 0.04	-0.69 ± 0.12
15/2	from +0.05 to -0.32 or from -3.0 to -16.0	0.20 ± 0.04	-0.82 ± 0.15
17/2		0.22 ± 0.04	0.72 ± 0.12[a])
21/2		0.23 ± 0.05	0.63 ± 0.13[a])

a) The negative value of the mixing amplitude was adopted in analogy with the four lower-lying levels.

Table 6

Isotope	Experiment		Theory	Difference
Hf 171	7/2	0	0.9	+0.9
	9	61.7	61.4	-0.3
	11	145.9	147.6	+1.7
	13	244.9	245.5	+0.6
	15	381.9	383.6	+1.7
	17	511.8	513.7	+1.9
	19	715.6	713.2	-2.4
	21	865.2	866.2	+1.0
	23	1144.4	1139.0	-5.4
	25	1305.0	1303.0	-2.0
	27	1660.5	1662.5	+2.0
	29	1825.7	1826.1	+0.4
		Δ_{rms} = 0.615	Δ_{av} = 1.68	
Hf 173	7	197.7	198.4	+0.7
	9	255.7	257.8	+2.1
	11	337.2	338.9	+1.7
	13	436.8	439.7	+2.9
	15	568.8	568.2	-0.6
	17	705.6	708.6	+3.0
	19	897.5	891.1	-6.4
	21	1061.1	1062.9	+1.8
	23	1318.6	1310.5	-8.1
	25	1499.2	1497.8	-1.4
	27	1823.8	1828.1	+4.3
		Δ_{rms} = 1.132	Δ_{av} = 2.9	

Table 6 (continued)

Isotope		Experiment	Theory	Difference
Hf 175	7	207.4	206.6	+0.8
	9	257.9	257.6	-0.3
	11	335.9	336.8	+1.6
	13	436.0	436.9	+0.9
	15	566.2	567.8	+1.6
	17	710.8	710.8	0.0
	19	896.9	895.4	-1.5
	21	1075.7	1073.4	-2.3
	23	1322.7	1319.4	-3.3
	25	1523.3	1524.4	+1.1
	27	1837.1	1840.2	+3.1
		$\Delta_{rms} = 0.546$	$\Delta_{av} = 1.51$	
Hf 177	9	321.3	321.1	-0.2
	11	426.6	427.1	+0.5
	13	555.0	555.6	+0.6
	15	708.2	707.4	+0.8
	17	882.6	883.0	+0.4
	19	1086.7	1083.2	-3.5
	21	1301.2	1307.9	+6.7
	23	1560.9	1558.2	-2.7
	7	747.2	750.0	+2.8
	9	849.1	845.4	-3.7
		$\Delta_{rms} = 0.936$	$\Delta_{av} = 2.19$	

Table 6 (continued)

Isotope	Experiment		Theory	Difference
Hf 179	9	0	0.7	+0.7
	11	122.7	123.0	+0.3
	13	268.9	269.6	+0.7
	15	438.7	439.0	+0.3
	17	631.5	631.5	0.0
	19	848.5	847.1	-1.4
	21	1085.2	1086.0	+0.8
		$\Delta_{rms} = 0.277$	$\Delta_{av} = 0.61$	

Table 7

Parameters Used in Hf Isotopes Energy Level Fits

Number of Parameters Varied*	Isotope	$\frac{\hbar^2}{2J}$ (keV)	a	α	E_p (keV)	E_h (keV)	nG_h (keV)	nG_p (keV)
5	171	12.78	[7.105]	0.597	+378.9	-168.9	(-422)	(-105)
7	173	12.74	8.27	0.598	+ 33.63	-266.4	-426	-346
6	175	12.33	6.230	0.491	+210.0	-381.5	(-543)	(-724)
7	177	13.81	6.349	0.669	+1594.5	-195.9	-460	-362
5	179	12.50	[6.181]	0.424	+122.0	+ 63.7	(-397)	(-298)

*Quantities in square brackets were not varied. Theoretical values were used as stated in the text. Quantities in parentheses were constrained to vary in fixed ratio to one another, the ratio being fixed by theoretical considerations regarding numbers of orbitals available near the Fermi surface.

FIGURE CAPTIONS

Fig. 1. The γ-ray spectrum produced in the bombardment of the ^{170}Yb target with 38 MeV α-particles. The energies of γ-lines are given in keV. The γ-lines with the given energies belong to ^{171}Hf unless stated otherwise.

Fig. 2. The γ-ray spectrum produced in the bombardment of the ^{165}Ho target with 52 MeV ^{10}B ions. The energies of the γ-lines are given in keV. The γ-lines with the given energies belong to ^{171}Hf unless stated otherwise.

Fig. 3. Some coincidence spectra restored from the experiment with ^{10}B on ^{165}Ho target. The gross coincidence spectrum shown in the upper part of the picture is a spectrum in coincidence with all events in the other detector. The three spectra in the lower part of the graph are coincident with the full-energy peak of the γ-line specified, i.e., the contributions of coincidences with the pedestals were subtracted. See Table 3 for summary.

Fig. 4. The part of ^{171}Hf level scheme populated from ^{171}Ta decay which is relevant to the level assignment from the in-beam experiments. This partial decay scheme was obtained from the study now in progress at the Yale Heavy Ion Accelerator Laboratory.

Fig. 5. The level scheme of ^{171}Hf determined in this study. The level and transition energies are in keV. The transitions marked with asterisk were placed each in two positions of the level scheme. When a dot was placed between two transitions it means that the coincidence relation between these two transitions was established: heavy dots mark those relationships determined in this study in ^{165}Ho(^{10}B,4n) reaction; open circles indicate that the coincidence was established from the decay study of ^{171}Ta. Few transitions from the latter study were included into this level scheme and are shown here in italics.

Fig. 6. The dependence of $[E(I) - E(I-1)]/2I$ on the square of level spin for the $5/2^-[512]$ and $7/2^+[633]$ bands in ^{171}Hf. The solid line for the $7/2^+$ band is the result of the power series fits with eq. 1.

Fig. 7. Scheme for constructing of the "supermatrix" in the case of ^{177}Hf. In the lower part of the figure, the diagram of the tenth state in the 10×10 supermatrix above is shown. See also text for discussion.

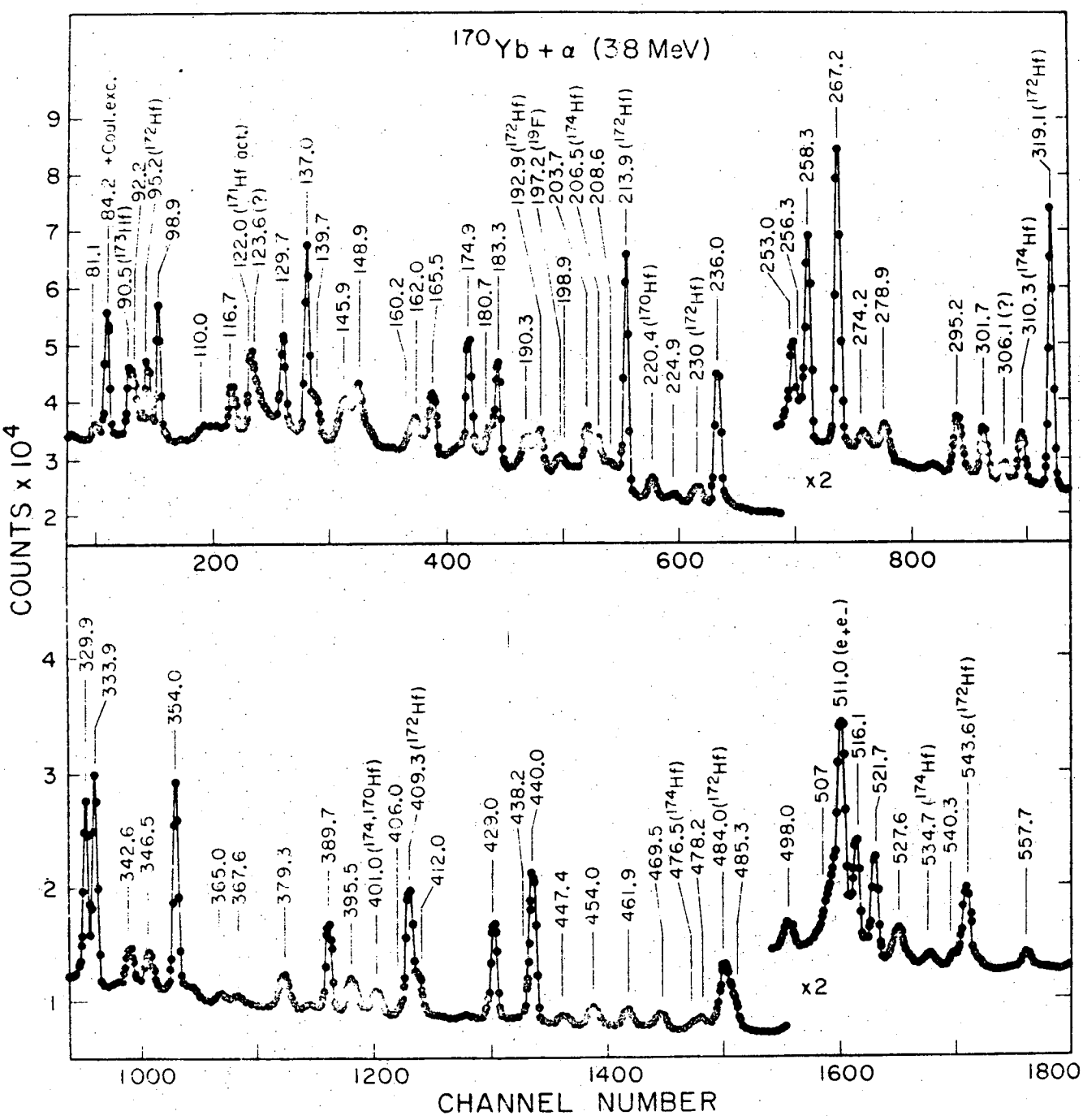
^{170}Yb + α (38 MeV)
COUNTS x 10^4
CHANNEL NUMBER
81.1
84.2 +Coul.exc.
90.5(^{173}Hf)
92.2
95.2(^{172}Hf)
98.9
110.0
116.7
122.0(^{171}Hf oct.)
123.6(?)
129.7
137.0
139.7
145.9
148.9
160.2
162.0
165.5
174.9
180.7
183.3
190.3
192.9(^{172}Hf)
197.2(^{19}F)
203.7
198.9
206.5(^{174}Hf)
208.6
213.9(^{172}Hf)
220.4(^{170}Hf)
224.9
230(^{172}Hf)
236.0
253.0
256.3
258.3
267.2
274.2
278.9
295.2
301.7
306.1(?)
310.3(^{174}Hf)
319.1(^{172}Hf)
x2
329.9
333.9
342.6
346.5
354.0
365.0
367.6
379.3
389.7
395.5
401.0(^{174,170}Hf)
406.0
409.3(^{172}Hf)
412.0
429.0
438.2
440.0
447.4
454.0
461.9
469.5
476.5(^{174}Hf)
478.2
484.0(^{172}Hf)
485.3
498.0
507
511.0 (e$^+$e$^-$)
516.1
521.7
527.6
534.7 (^{174}Hf)
540.3
543.6(^{172}Hf)
557.7
x2

Figure 1

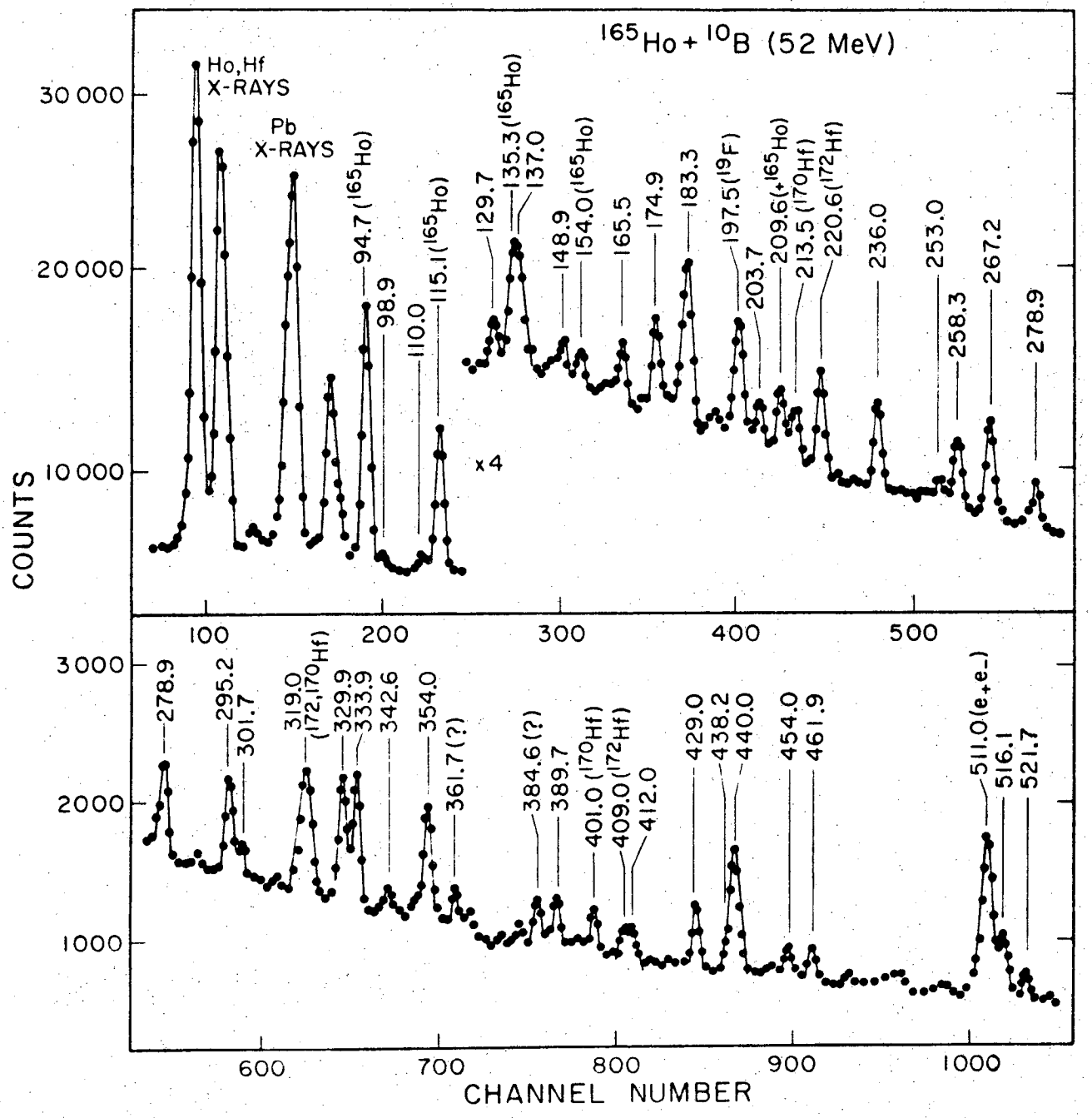
^{165}Ho + ^{10}B (52 MeV)
Ho,Hf X-RAYS
Pb X-RAYS
94.7 (^{165}Ho)
98.9
110.0
115.1 (^{165}Ho)
129.7
135.3 (^{165}Ho)
137.0
148.9
154.0 (^{165}Ho)
165.5
174.9
183.3
197.5 (^{19}F)
203.7
209.6 (+^{165}Ho)
213.5 (^{170}Hf)
220.6 (^{172}Hf)
236.0
253.0
258.3
267.2
278.9
x4
COUNTS
30 000
20 000
10 000
3000
2000
1000
100
200
300
400
500
278.9
295.2
301.7
319.0 (^{172,170}Hf)
329.9
333.9
342.6
354.0
361.7 (?)
384.6 (?)
389.7
401.0 (^{170}Hf)
409.0 (^{172}Hf)
412.0
429.0
438.2
440.0
454.0
461.9
511.0 (e+e-)
516.1
521.7
600
700
800
900
1000
CHANNEL NUMBER

Figure 2

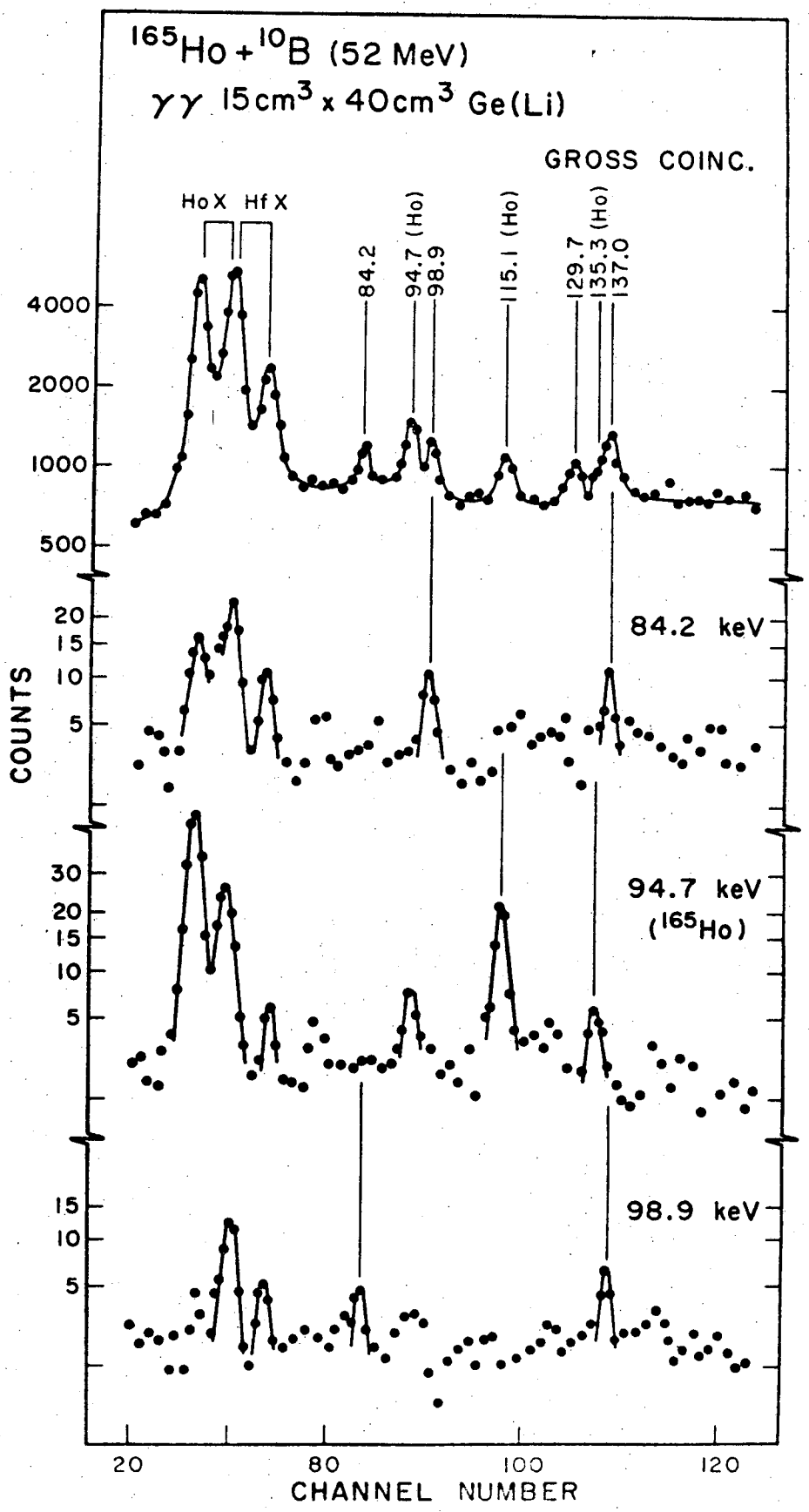
^{165}Ho + ^{10}B (52 MeV)
γγ 15cm^3 x 40cm^3 Ge(Li)
GROSS COINC.
Ho X
Hf X
84.2
94.7 (Ho)
98.9
115.1 (Ho)
129.7
135.3 (Ho)
137.0
4000
2000
1000
500
84.2 keV
94.7 keV
(^{165}Ho)
98.9 keV
COUNTS
20
80
100
120
CHANNEL NUMBER

Figure 3

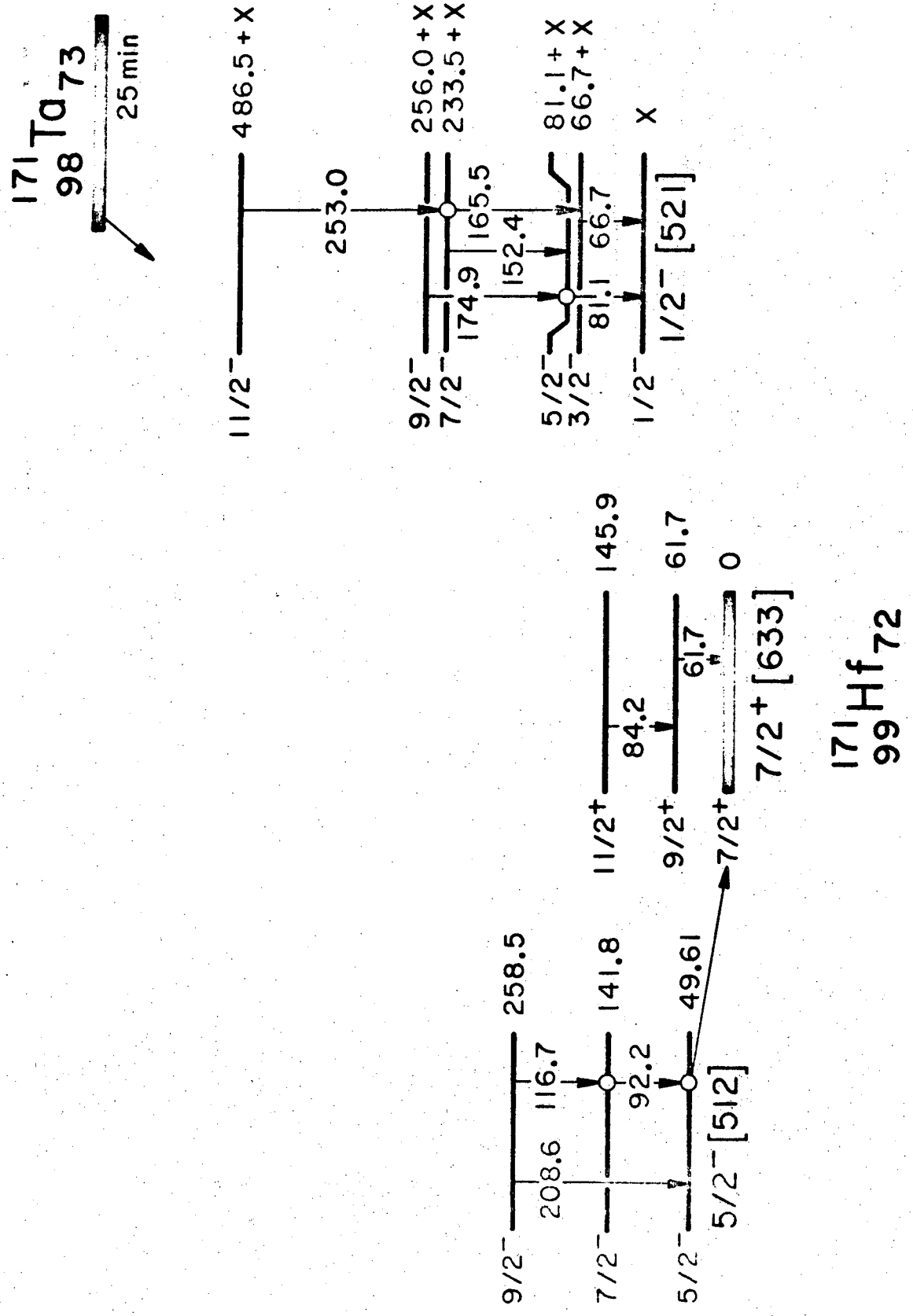
171 98 Ta 73
25 min
486.5 + X
256.0 + X
233.5 + X
81.1 + X
66.7 + X
X
253.0
165.5
152.4
174.9
66.7
81.1
11/2−
9/2−
7/2−
5/2−
3/2−
1/2−
1/2− [521]
145.9
61.7
0
84.2
61.7
11/2+
9/2+
7/2+
7/2+ [633]
171 99 Hf 72
258.5
141.8
49.61
116.7
92.2
208.6
9/2−
7/2−
5/2−
5/2− [512]

Figure 4

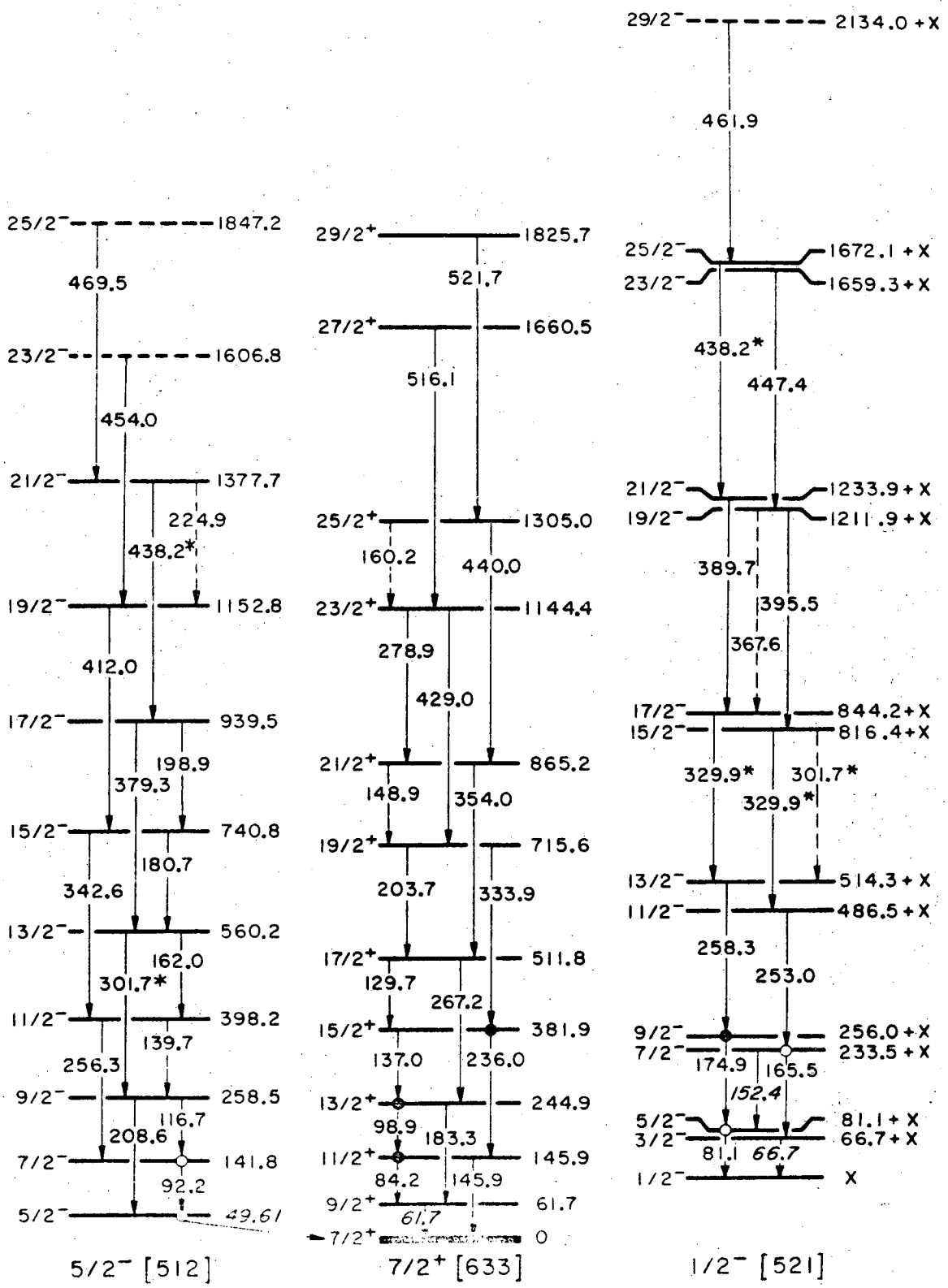

$^{171}_{99}Hf_{72}$

Figure 5

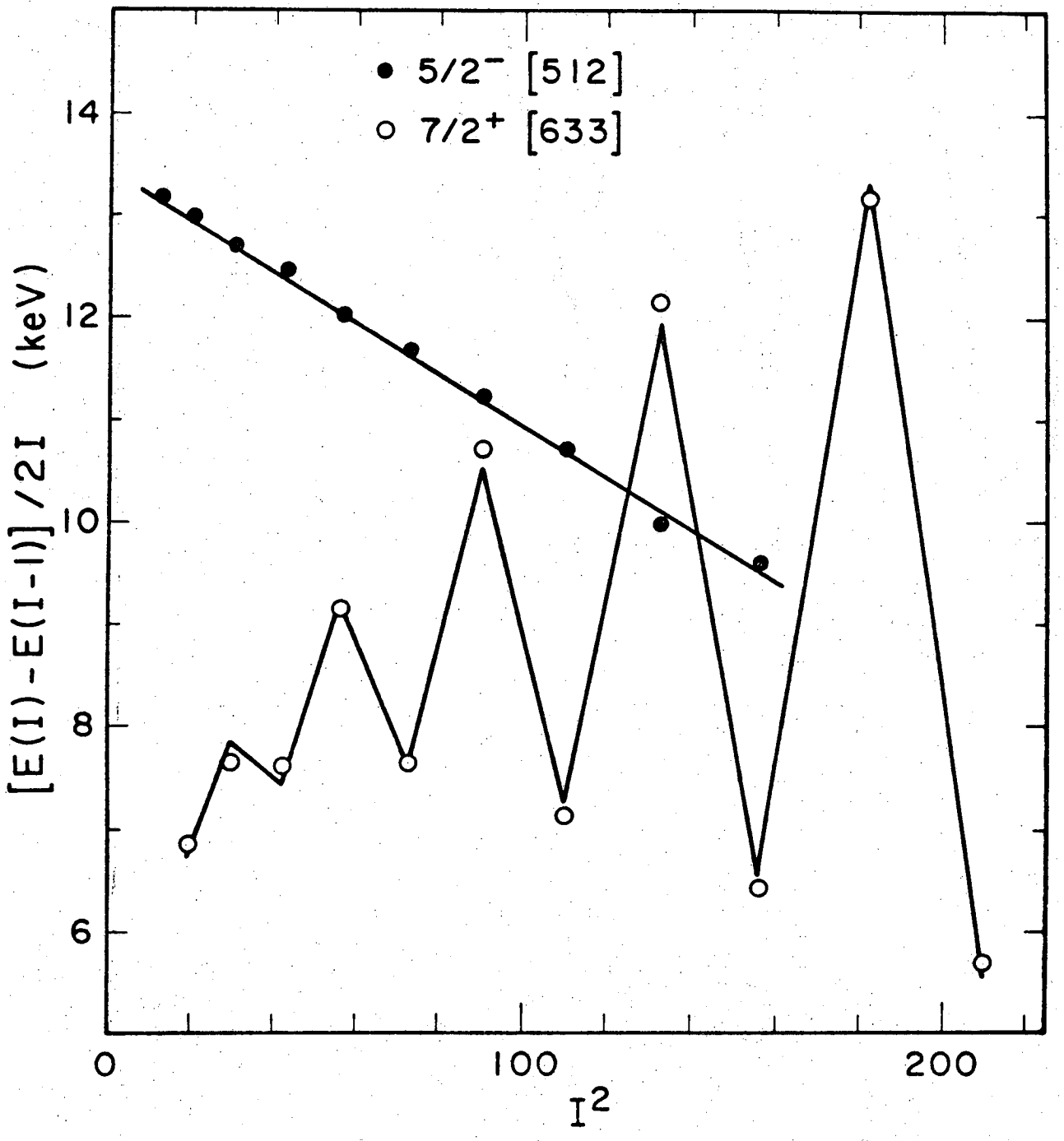

Figure 6

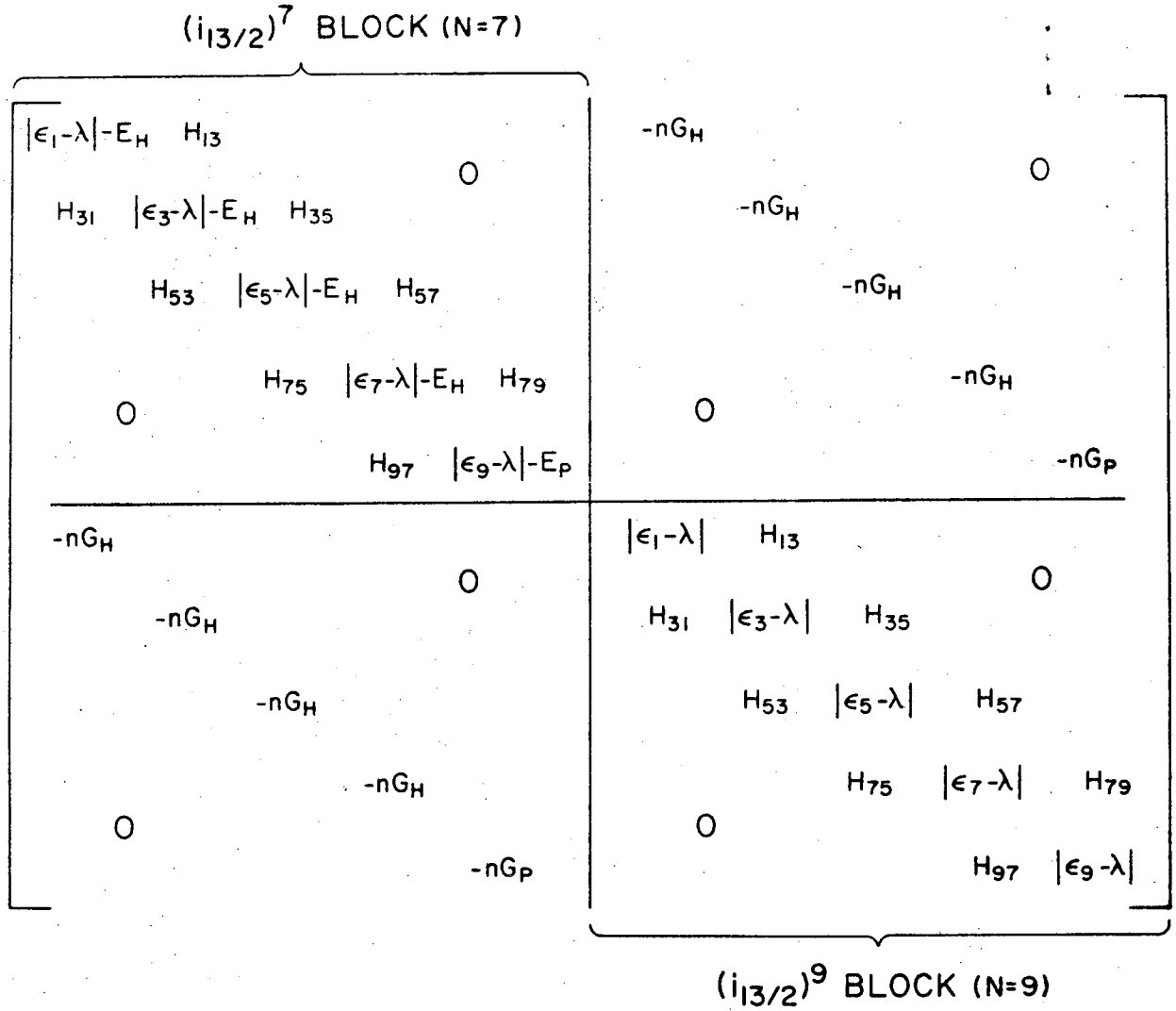
$(i_{13/2})^7$ BLOCK (N=7)
$|\epsilon_1-\lambda|-E_H$ H_{13}
H_{31} $|\epsilon_3-\lambda|-E_H$ H_{35}
H_{53} $|\epsilon_5-\lambda|-E_H$ H_{57}
H_{75} $|\epsilon_7-\lambda|-E_H$ H_{79}
H_{97} $|\epsilon_9-\lambda|-E_P$
$-nG_H$
$-nG_P$
$|\epsilon_1-\lambda|$ H_{13}
H_{31} $|\epsilon_3-\lambda|$ H_{35}
H_{53} $|\epsilon_5-\lambda|$ H_{57}
H_{75} $|\epsilon_7-\lambda|$ H_{79}
H_{97} $|\epsilon_9-\lambda|$
$(i_{13/2})^9$ BLOCK (N=9)

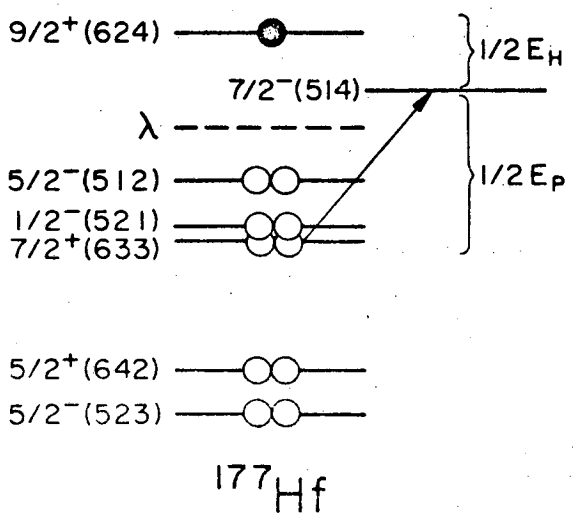
$9/2^+(624)$
$7/2^-(514)$
λ
$5/2^-(512)$
$1/2^-(521)$
$7/2^+(633)$
$1/2\,E_H$
$1/2\,E_P$
$5/2^+(642)$
$5/2^-(523)$
^{177}Hf

Figure 7

TECHNICAL INFORMATION DIVISION
LAWRENCE BERKELEY LABORATORY
UNIVERSITY OF CALIFORNIA
BERKELEY, CALIFORNIA 94720